Sheared Poloidal Flow Driven by Mode Conversion in Tokamak Plasmas

E. F. Jaeger,[1] L. A. Berry,[1] J. R. Myra,[2] D. B. Batchelor,[1] E. D'Azevedo,[1] P. T. Bonoli,[3] C. K. Phillips,[4] D. N. Smithe,[5] D. A. D'Ippolito,[2] M. D. Carter,[1] R. J. Dumont,[4] J. C. Wright,[3] and R. W. Harvey[6]

[1]*Oak Ridge National Laboratory, Oak Ridge, Tennessee 37831-8071, USA*
[2]*Lodestar Research Corporation, 2400 Central Avenue P-5, Boulder, Colorado 80301, USA*
[3]*Plasma Fusion Center, Massachusetts Institute of Technology, Cambridge, Massachusetts 02139, USA*
[4]*Princeton Plasma Physics Laboratory, P.O. Box 451, Princeton, New Jersey 08543, USA*
[5]*Mission Research Corporation, 8560 Cinderbed Road, Suite 700, Newington, Virginia 22122-8560, USA*
[6]*CompX, P.O. Box 2672, Del Mar, California 92014-5672, USA*

(Received 23 January 2003; published 13 May 2003)

A two-dimensional integral full-wave model is used to calculate poloidal forces driven by mode conversion in tokamak plasmas. In the presence of a poloidal magnetic field, mode conversion near the ion-ion hybrid resonance is dominated by a transition from the fast magnetosonic wave to the slow ion cyclotron wave. The poloidal field generates strong variations in the parallel wave spectrum that cause wave damping in a narrow layer near the mode conversion surface. The resulting poloidal forces in this layer drive sheared poloidal flows comparable to those in direct launch ion Bernstein wave experiments.

DOI: 10.1103/PhysRevLett.90.195001 PACS numbers: 52.50.Qt, 52.35.Ra, 52.55.Fa

Recent experiments on the Tokamak Fusion Test Reactor (TFTR) [1] have shown that directly coupled ion Bernstein waves (IBW) can be used to drive sheared poloidal flow at high cyclotron harmonics in a tokamak plasma. In addition, experiments on the Frascati Tokamak Upgrade (FTU) [2], along with several calculations [3–6], suggest that these externally driven sheared flows can trigger internal transport barriers that reduce microturbulence and enhance plasma confinement. Unfortunately, the technology required for direct coupling of IBW to the bulk plasma is extremely difficult and not fully understood. A simpler and perhaps more efficient means of driving sheared flow would be to use mode conversion. Mode conversion in radio frequency (rf) heated plasmas has been the subject of both theoretical [7–10] and experimental [11–15] studies. Previous one-dimensional (1D) simulations of mode conversion [16–19] near the ion-ion hybrid resonance show a transition from the fast magnetosonic wave to the slow IBW. In standard light ion minority scenarios (low m/Z) without a poloidal magnetic field, IBW propagates on the high field side of the ion-ion hybrid resonance and is absorbed by electron Landau damping and transit time magnetic pumping. By themselves, these mechanisms do not lead to poloidal flow [4]. Hence, there is no significant flow drive associated with mode conversion. Recently, however, two-dimensional (2D) calculations [10] have shown that the mode conversion process is significantly modified when a poloidal field is present. Two-dimensional calculations give a much more complete understanding of the various mode conversion processes at work in real tokamaks than do previous 1D models.

In this Letter, we apply a 2D integral full-wave model [10] to calculate the poloidal forces resulting from mode conversion near the ion-ion hybrid resonance. In the presence of a poloidal magnetic field, mode conversion is dominated by a transition from the fast magnetosonic wave to the slow ion cyclotron wave (ICW). Unlike the mode-converted ion Bernstein wave, the ICW is a cold plasma wave that usually propagates on the low field side of the mode conversion layer. The poloidal magnetic field generates strong variations in the parallel wave number ($k_\parallel$) that broaden the cyclotron resonance and allow damping of the ICW by both ions and electrons in a narrow layer near the mode conversion surface. The resulting poloidal forces in this layer can drive sheared poloidal flows. In recent experiments [14,15], both ion absorption and poloidal flow have been observed near the mode conversion layer. The possibility of mode conversion to the ICW was first suggested in 1977 by Perkins [7] and has recently been observed both numerically [10] and experimentally [13]. However, the 2D effect of the poloidal field on the mode-converted ICW and the resulting sheared poloidal flow have not previously been analyzed.

For time-harmonic wave fields with frequency ω, Maxwell's equations combine to give the inhomogeneous wave equation [8],

$$-\nabla \times \nabla \times \mathbf{E} + k_0^2 \left(\mathbf{E} + \frac{i}{\omega \epsilon_0} \mathbf{J}_p \right) = -i\omega \mu_0 \mathbf{J}_{\text{ant}}, \quad (1)$$

where $\mathbf{E}$ is the wave electric field, $\mathbf{J}_p$ is the plasma current, $\mathbf{J}_{\text{ant}}$ is the antenna current, and $k_0 = \omega/c$. Tokamak geometry is described in terms of toroidal coordinates R, Z, and φ, where R is the radial position measured from the toroidal axis, Z is the vertical position measured from the midplane, and φ is the toroidal angle. The relationship between the plasma current and the wave electric field is nonlocal, and can be expressed to lowest order as an integral operator of the form [20],

$$\mathbf{J}_p(\mathbf{r}) = \int d\mathbf{r}' \sigma(\mathbf{r}, \mathbf{r}' - \mathbf{r}) \cdot \mathbf{E}(\mathbf{r}'), \quad (2)$$

where $\mathbf{r}$ is the position vector, and σ is the plasma conductivity [8].

Numerical solutions of Eqs. (1) and (2) have been carried out using AORSA [10], a fully spectral 2D full-wave model. AORSA includes the complete integral representation of the plasma current in Eq. (2), makes no assumption regarding the smallness of $k_\perp \rho$ ($k_\perp$ is the perpendicular wave number, and ρ is the ion Larmor radius), and imposes no limit on the number of cyclotron harmonics. Because all modes in the spectral representation are coupled, AORSA requires the inversion of a large, dense matrix, and is therefore computationally more intensive than previous codes using finite Larmor radius (FLR) expansions such as PICES [21] and TORIC [22].

In Fig. 1, AORSA is used to simulate mode conversion near the ion-ion hybrid layer in Alcator C-Mod [12,13]. The plasma consists of deuterium ions with 23% He^3 and 33% H. Figure 1(a) shows contours of the perpendicular rf electric field. Vertical lines indicate the location of the ion-ion hybrid (left) and ion cyclotron resonances (right) for both He^3 and H. In Fig. 1(b), the mode conversion region is expanded to show contours of the real part of the parallel electric field $E_\parallel$. Notice that over most of the plasma cross section, the mode-converted waves propagate on the low field side (right) of the ion-ion hybrid resonance, with wavelength decreasing to the right. However, for the region immediately surrounding the magnetic axis, the opposite is true.

The poloidal magnetic field has a profound effect on the mode conversion process itself and on the interaction between the mode-converted waves and the plasma. In Fig. 2, three different values of normalized poloidal field (b_p) are shown for the He^3-H-D mode conversion scenario. Solid lines show the location of the ion-ion hybrid resonance. For $b_p = 0$, the mode-converted wave (IBW) propagates on the high field side (left) of the mode conversion surface in agreement with previous 1D results without a poloidal field. As the poloidal field is increased in Fig. 2(b), a new wave (ICW) appears on the low field side of the resonance. For poloidal field magnitudes typical of real tokamaks as in Fig. 2(c), this new wave dominates the mode conversion process, except for the region immediately surrounding the magnetic axis.

In Fig. 2, dispersion solutions are shown for different values of b_p corresponding to the 2D plasma locations indicated by the arrows. Assuming $\mathbf{k} \cdot \hat{\mathbf{e}}_Z = 0$ for the dispersion analysis, $k_\parallel$ can be written in terms of $k_\perp$ as

$$k_\parallel = \frac{1}{b_T}(b_p k_\perp + k_\varphi). \tag{3}$$

This dependence of $k_\parallel$ on $k_\perp$ reflects the "up-shift" and

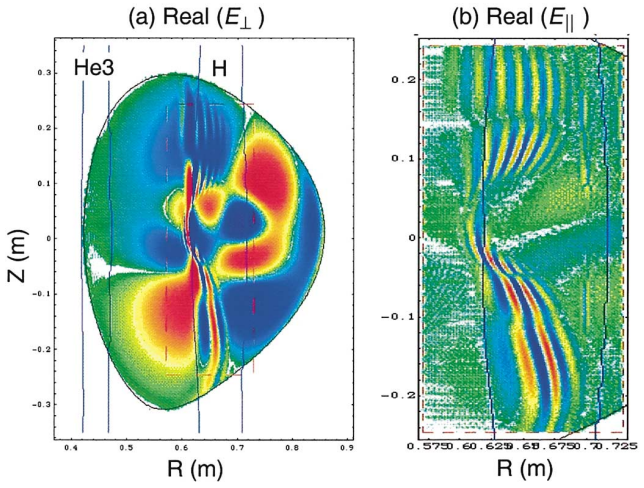

FIG. 1 (color). He^3-H-D mode conversion in Alcator C-Mod [12,13] with $B_0 = 5.85$ T and $n_\phi = 10$ from AORSA.

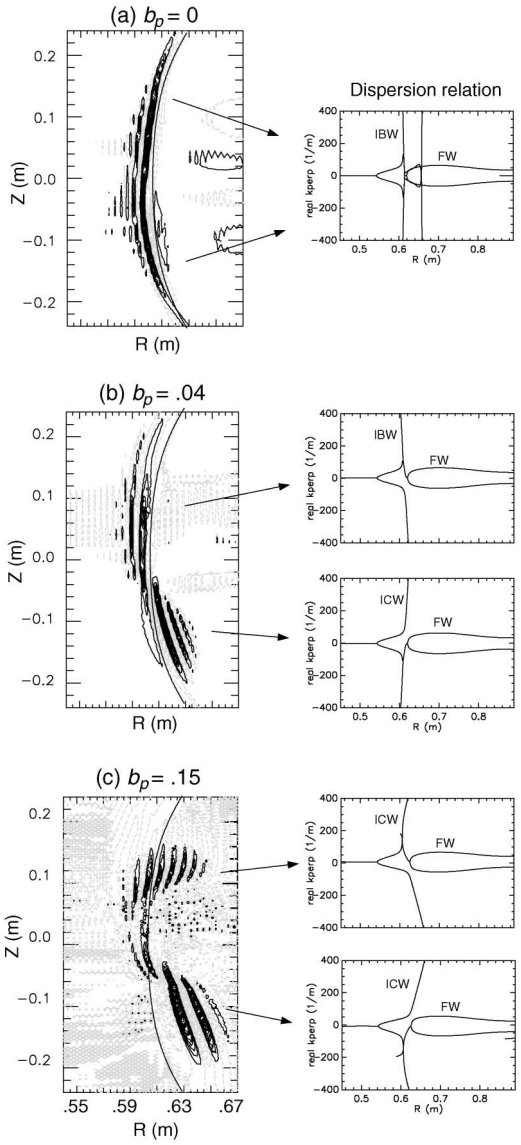

FIG. 2. Effect of the poloidal magnetic field b_p for He^3-H-D mode conversion with $n_\varphi = 15$ from AORSA [10].

"down-shift" that occurs in $k_\parallel$ when waves propagate in a poloidal magnetic field [23]. The phase velocity of the mode-converted waves in Fig. 2 is positive in x. Thus the relevant part of the dispersion plots is the upper half plane where $k_\perp > 0$. In all cases, the 1D dispersion results agree qualitatively with the 2D calculations. Different dispersion behavior is observed, depending on the amount of up-shift and down-shift in $k_\parallel$. For example, in Fig. 2(b), the two terms in Eq. (3) are comparable in magnitude. When they subtract as above the midplane in Fig. 2(b), $k_\parallel$ is down-shifted and the waves propagate to the left of the resonance. When they add as below the midplane in Fig. 2(b), $k_\parallel$ is up-shifted, and the waves propagate to the right of the resonance. For larger values of poloidal field as in Fig. 2(c), the variation in $k_\parallel$ is dominated by the first term in Eq. (3) and is proportional to b_p. In this case, the mode-converted wave is approximately independent of the sign of b_p because the dispersion relation depends to lowest order on $k_\parallel^2$, or from Eq. (3) on b_p^2. Thus we see similar behavior above and below the midplane.

If the calculations in Fig. 2 are repeated for a very low ion temperature, we find that on the low field side of the ion-ion hybrid resonance, the mode-converted waves are cold plasma, forward waves consistent with ICW. On the high field side, they are predominantly finite temperature, backward waves consistent with IBW. It is clear from Figs. 1 and 2 that some amount of up-shift in $k_\parallel$ is necessary for the mode-converted ICW to propagate. This is consistent with cold plasma theory. Near the magnetic axis, where the poloidal field is small, the up-shift in $k_\parallel$ is not large enough to support ICW. However, IBW propagates easily in this region.

These results also depend on a relatively high minority ion concentration. As the fraction of minority ions is reduced, FLR effects become more important at the mode conversion layer, and the IBW near the magnetic axis becomes stronger as shown in Fig. 3.

The interaction between the plasma and the mode-converted ICW leads to wave damping in a narrow layer near the mode conversion surface. Terms that give rise to this damping are enhanced by the up-shift in $k_\parallel$ caused by the poloidal magnetic field, and the resulting poloidal forces drive sheared poloidal flow in the mode conversion layer. The calculation of the perpendicular force exerted by the waves on the plasma [4–6] can be generalized to two spatial dimensions. To lowest order in spectral width [5], the direct force $\mathbf{F}^{(0)}$ exerted by the waves on the plasma can be written as the sum of the wave momentum for each Fourier component $(\mathbf{k}/\omega)$ times the power absorbed in that component. This force contains a dissipative part corresponding to the absorption of photon momentum,

$$\mathbf{F}_1^{(0)} = \mathrm{Re} \sum_{\mathbf{k}_R,\mathbf{k}_L} \frac{\mathbf{k}_L + \mathbf{k}_R}{4\omega} e^{i(\mathbf{k}_R - \mathbf{k}_L)\cdot\mathbf{r}} \sum_l e^{il(\vartheta_R - \vartheta_L)} \varepsilon_{k_L}^* \cdot \mathbf{H}_l \cdot \varepsilon_{k_R} \tag{4}$$

and a reactive part that reduces to the ponderomotive force in the cold plasma limit [6,24],

$$\mathbf{F}_2^{(0)} = \mathrm{Re} \sum_{\mathbf{k}_R,\mathbf{k}_L} \frac{\mathbf{k}_L - \mathbf{k}_R}{4\omega} e^{i(\mathbf{k}_R - \mathbf{k}_L)\cdot\mathbf{r}} \sum_l e^{il(\vartheta_R - \vartheta_L)} \varepsilon_{k_L}^* \cdot \mathbf{A}_l \cdot \varepsilon_{k_R}, \tag{5}$$

where $\mathbf{H}_l$ and $\mathbf{A}_l$ are, respectively, the Hermitian and anti-Hermitian parts of the tensor $\mathbf{W}_l$ given in Eq. (16) of Ref. [5]. In Eqs. (4) and (5), ε_k is the Fourier component of the rf electric field in local magnetic coordinates [8],

$$\begin{aligned} \varepsilon_{x,k} &= E_{x,k}\cos\vartheta + E_{y,k}\sin\vartheta, \\ \varepsilon_{y,k} &= E_{y,k}\cos\vartheta - E_{x,k}\sin\vartheta, \\ \varepsilon_{z,k} &= E_{z,k}, \end{aligned} \tag{6}$$

where ϑ is the angle between $\mathbf{k}_\perp$ and the local unit vector $\hat{\mathbf{e}}_\alpha$ (the component of $\hat{\mathbf{e}}_x$ perpendicular to $\mathbf{B}$). The reactive part of the force, $\mathbf{F}_2^{(0)}$, tends to be locally large, but does not drive flux surface average flows because $\mathbf{k}_L - \mathbf{k}_R$ in Eq. (5) corresponds to a gradient operator in configuration space, and the relevant flux surface averages are zero.

To next order, there are additional forces due to the transport of momentum [4–6]. These can be written as

$$\mathbf{F}^{(1)} = \frac{1}{4\boldsymbol{\Omega}} \mathrm{Re} \int d^3v [\hat{\mathbf{b}} \times \nabla(\mathbf{v}_\perp \cdot \mathbf{F}_{\mathrm{EM}}^*) - \nabla(\hat{\mathbf{b}}\cdot\mathbf{v} \times \mathbf{F}_{\mathrm{EM}}^*)], \tag{7}$$

where $\mathbf{F}_{EM}$ is the electromagnetic force due to the waves, weighted by the first order distribution function. The first term in Eq. (7) corresponds to the 1D force calculated in Refs. [4–6]. For the example given below, this force is more than an order of magnitude smaller than the direct dissipative part in Eq. (4). Also, the second term in Eq. (7) vanishes under a flux surface average.

Figure 4(a) shows 2D contour plots of the power absorbed and the dissipative part of the poloidal force for the minority ions in the example of Fig. 1. The absorption and poloidal force are skewed toward the lower half of the

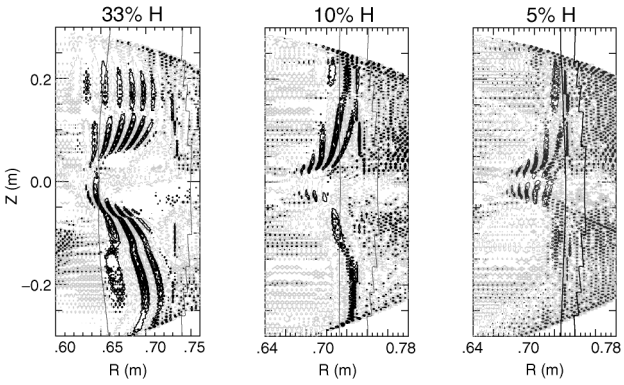

FIG. 3. Effect of the minority ion concentration for the He^3-H-D mode conversion scenario in Figs. 1 and 2.

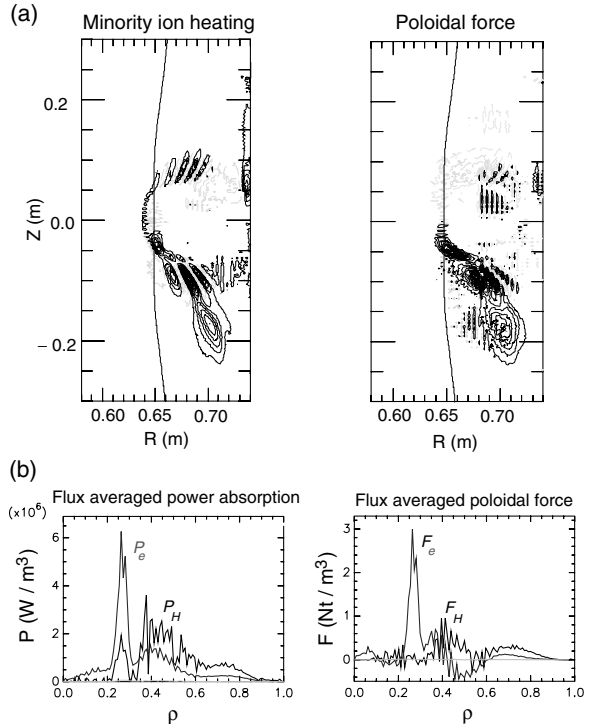

FIG. 4. (a) Contours of minority ion heating and poloidal force for the example in Fig. 1; (b) flux surface averaged power and poloidal force with 1 MW of rf power absorbed.

plasma where the sign of the poloidal field is such that the terms in Eq. (3) add to give up-shift in $k_{\|}$. This up-down asymmetry leads to poloidal forces from the direct term in Eq. (4), whereas in 1D, the direct force is zero. Figure 4(b) shows the flux surface average of the power absorption and poloidal force for electrons and minority ions. Note that the poloidal force on each species follows closely the power absorbed in that species. With 1 MW of total rf power, the magnitude of the peak force on the electrons is about 3 $\mathrm{Nt/m^3}$. This is comparable to the force calculated [5] when 0.36 MW of high harmonic IBW is launched directly in TFTR and absorbed at the fifth harmonic cyclotron resonance [1]. These results are consistent with recent experiments [14,15] and suggest that mode conversion to ICW can be used to drive sheared poloidal flow, thereby creating internal transport barriers and giving access to enhanced confinement regimes.

The authors wish to thank M. Porkolab, F.W. Perkins, E. Nelson-Melby, O. Sauter, J. Vaclavik, and K. Appert for helpful discussions. Research was sponsored by Oak Ridge National Laboratory, managed by UT-Battelle, LLC, for the U.S. Department of Energy under Contract No. DE-AC05-00OR22725.

[1] B. P. LeBlanc *et al.*, Phys. Rev. Lett. **82**, 331 (1999).
[2] R. Cesario *et al.*, in *Radio Frequency Power in Plasmas*, edited by S. Bernabei and F. Paoletti, AIP Conf. Proc. No. 485 (AIP, New York, 1999), p. 100.
[3] H. Biglari, P. H. Diamond, and P. W. Terry, Phys. Fluids B **2**, 1 (1990).
[4] L. A. Berry, E. F. Jaeger, and D. B. Batchelor, Phys. Rev. Lett. **82**, 1871 (1999).
[5] E. F. Jaeger, L. A. Berry, and D. B. Batchelor, Phys. Plasmas **7**, 3319 (2000).
[6] J. R. Myra and D. A. D'Ippolito, Phys. Plasmas **7**, 3600 (2000).
[7] F.W. Perkins, Nucl. Fusion **17**, 1197 (1977).
[8] T. H. Stix, *Waves in Plasmas* (American Institute of Physics, New York, 1992), pp. 250–256.
[9] R. Majeski, C. K. Phillips, and J. R. Wilson, Phys. Rev. Lett. **73**, 2204 (1994).
[10] E. F. Jaeger *et al.*, Phys. Plasmas **8**, 1573 (2001).
[11] R. Majeski *et al.*, Phys. Rev. Lett. **76**, 764 (1996).
[12] P. T. Bonoli *et al.*, Phys. Plasmas **7**, 1886 (2000).
[13] E. Nelson-Melby *et al.*, Phys. Rev. Lett. **90**, 155004 (2003).
[14] C. K. Phillips *et al.*, Nucl. Fusion **40**, 461 (2000).
[15] C. Castaldo *et al.*, in *Proceedings of the 19th IAEA Fusion Energy Conference, Lyon, France, 2002* (IAEA, Vienna, 2002).
[16] P. L. Colestock and R. J. Kashuba, Nucl. Fusion **23**, 763 (1983).
[17] A. Fukuyama *et al.*, Nucl. Fusion **23**, 1005 (1983).
[18] H. Romero and J. Scharer, Nucl. Fusion **27**, 363 (1987).
[19] E. F. Jaeger, D. B. Batchelor, and H. Weitzner, Nucl. Fusion **28**, 53 (1988).
[20] M. Brambilla, *Kinetic Theory of Plasma Waves* (Clarendon Press, Oxford, 1998), pp. 18–20.
[21] E. F. Jaeger, D. B. Batchelor, and D. C. Stallings, Nucl. Fusion **33**, 179 (1993).
[22] M. Brambilla and T. Krucken, Nucl. Fusion **28**, 1813 (1988).
[23] A. K. Ram and A. Bers, Phys. Fluids B **3**, 1059 (1991).
[24] N. C. Lee and G. K. Parks, Phys. Fluids **26**, 724 (1983).